Electronic Supplementary Material (ESI) for Nanoscale.

Supporting information for

Subnano-transformation of Molybdenum Carbide to Oxycarbide

Masanori Wakizaka,[1] Augie Atqa,[1] Wang-Jae Chun,[2] Takane Imaoka,[1,*]

and Kimihisa Yamamoto[1,*]

[1]Laboratory for Chemistry and Life Science Institute of Innovative Research,

Tokyo Institute of Technology, Yokohama 226-8503, Japan

[2]Graduate School of Arts and Sciences, International Christian University, Tokyo 181-8585, Japan

Correspondence and requests for materials should be addressed to K.Y.

E-mail: yamamoto@res.titech.ac.jp

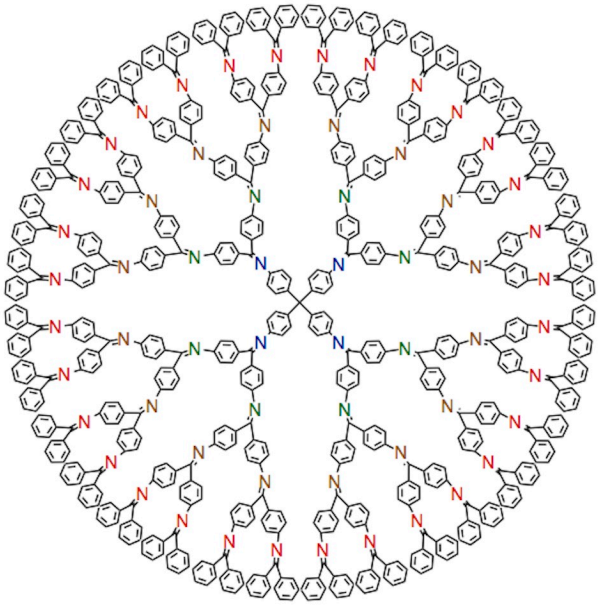

Figure S1. Chemical structure of the TPM-DPAG4 used for the cluster template.

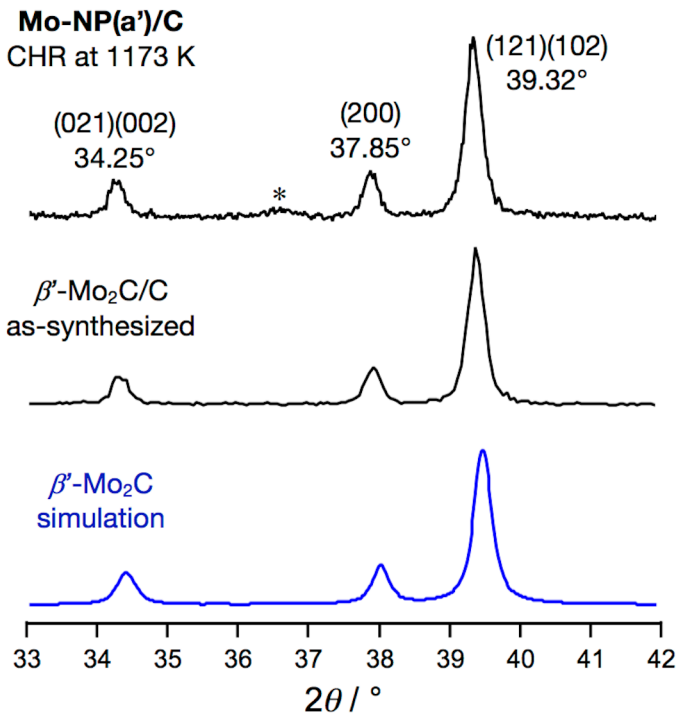

Figure S2. PXRD pattern of **Mo-NP(a')/C** after CHR at 1173 K for 3 h, β'-Mo_2C/C as-synthesized from MoO_3 and GMC by CHR at 1173 K for 1 h, and the simulation of β'-Mo_2C[S1,S2]. *The diffraction derived from a gas barrier film.

Equation S1. The crystal size (D) was estimated by Scherrer's equation, wherein K, λ, and β refer to the dimensionless shape factor = 0.9, the wavelength of x-ray, and the peak width at half the maximum intensity, respectively.

$$D = \frac{K\lambda}{\beta \cos\theta} \qquad \text{(Eq. S1)}$$

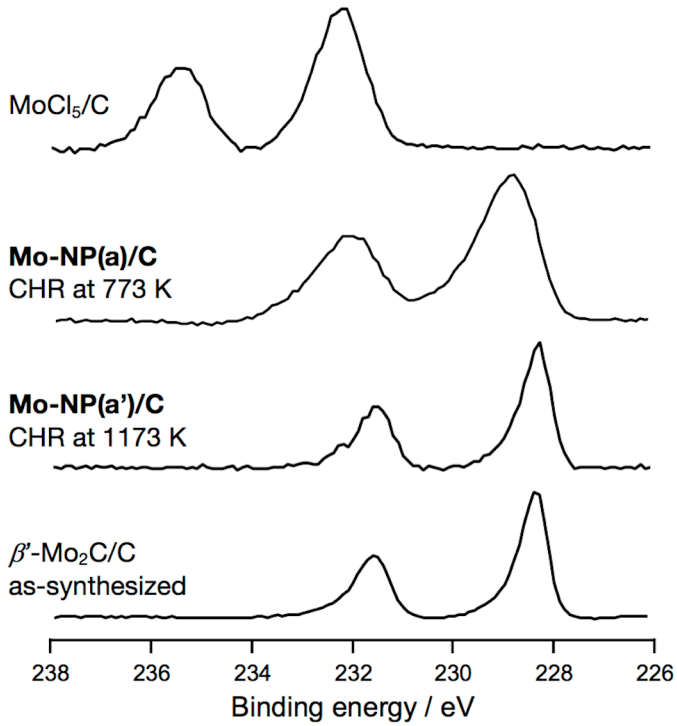

Figure S3. XPS spectra in the range of the binding energies for Mo $3d_{3/2}$ and $3d_{1/2}$ of $MoCl_5$/C, **Mo-NP(a)/C** after CHR at 773 K for 30 min, **Mo-NP(a')/C** after CHR at 1173 K for 3 h, and β'-Mo_2C/C as-synthesized from MoO_3 and GMC by CHR at 1173 K for 1 h. Binding energies were calibrated by setting the C 1s peak of GMC to 284.5 eV.

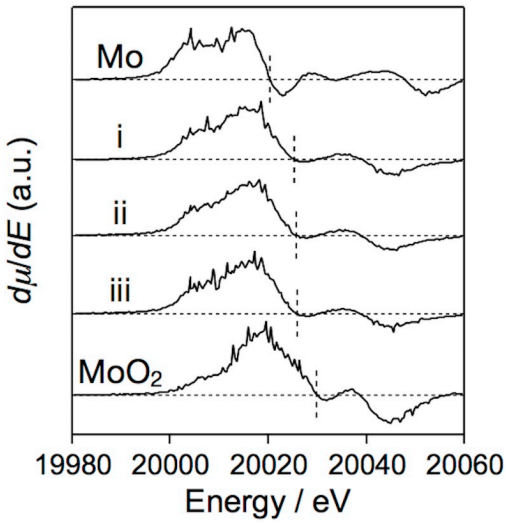

Figure S4. Mo–K edge XANES spectra of the first derivative for i) **Mo_{60}-aggregated/C**, ii) **Mo-NP(b)/C**, and iii) **Mo-NP(c)/C**, after CHR at 773 K for 30 min, along with those of Mo (foil) and MoO_2, measured using a Si(220) monochromator.

Table S1. Summary of the EXAFS curve fitting data

Sample	Pair	N	Distance / Å	σ^2 / 10^{-3} Å^2	ΔE_0 / eV	R_f / %
β'-Mo_2C	Mo–Mo	6 (set)	2.934[a] (set)	4.1±0.4	1.6±0.8	0.1
	Mo–Mo	6 (set)	3.014[b] (set)	3.8±0.4	–4.9±0.8	
Mo_{60}-aggregated/C	Mo–Mo	6.5±2.1	2.96±0.02	12.1±2.0	0.2±2.6	6.0
Mo foil	Mo–Mo	8 (set)	2.73±0.01	4.3±0.3	1.4±0.7	0.4
	Mo–Mo	6 (set)	3.15±0.01			

An inelastic reduction factor of $S_0^2 = 1.0$ for Mo–Mo was estimated from the amplitude of the Mo foil, in which the coordination numbers of bcc Mo are 8 and 6. All curve fitting was applied in k space (k = 3–14 Å^{-1}), and a Fourier filtering was applied in r = 2.1–3.0 (β'-Mo_2C), 1.75–3.0 (**Mo_{60}-aggregated/C**), and 1.8–3.4 (Mo foil), respectively. [a] The average distance obtained from shorter six Mo–Mo bonds in β'-Mo_2C, and [b] that obtained from longer six Mo–Mo bonds in β'-Mo_2C.[S1,S2]

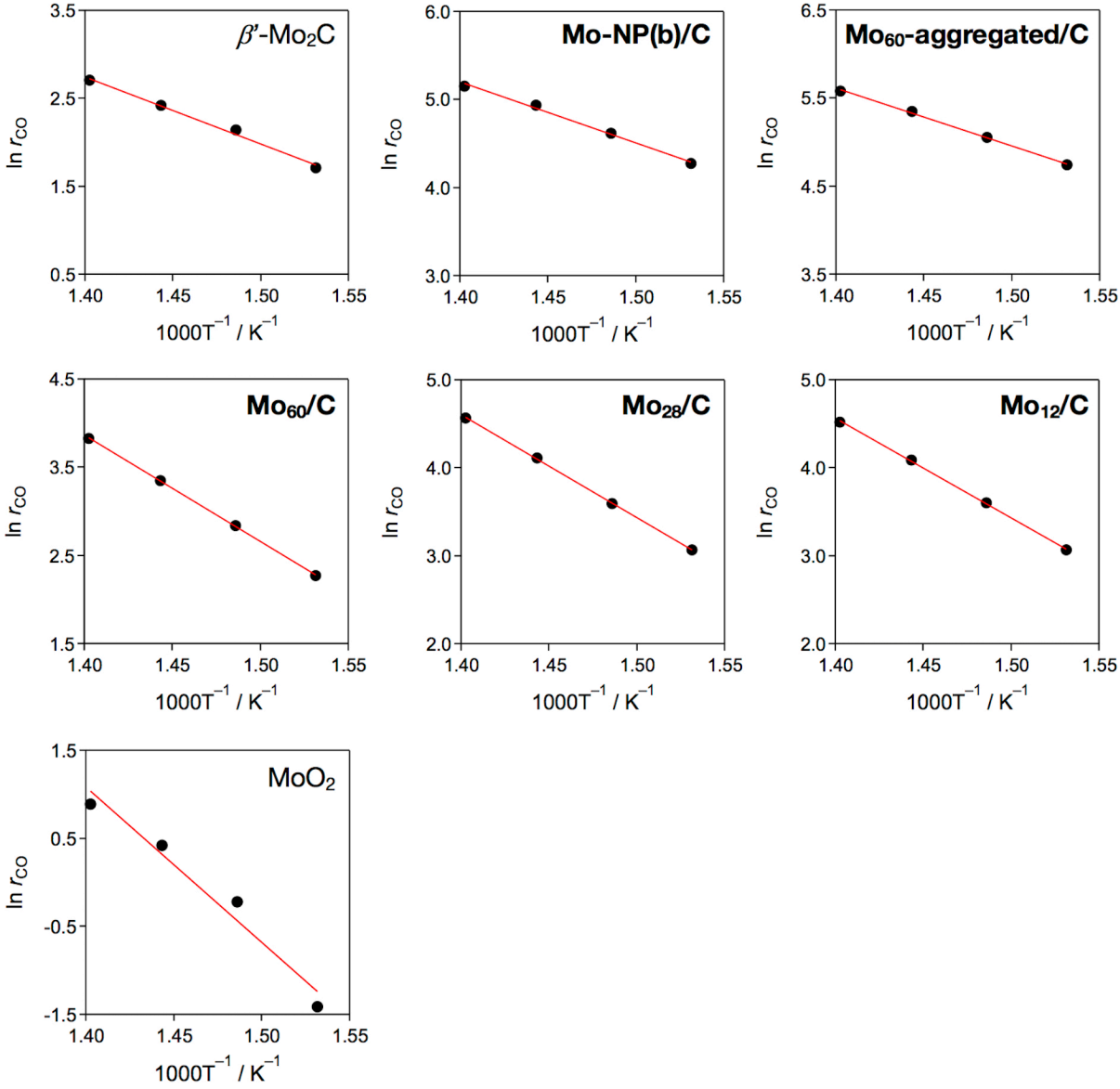

Figure S5. Arrhenius plots for RWGS reactions using β'-Mo_2C, **Mo-NP(b)/C**, **Mo_{60}-aggregated/C**, **Mo_{60}/C**, **Mo_{28}/C**, **Mo_{12}/C**, and MoO_2 as the catalyst under H_2/CO_2 (1/1, 1 atm) at 713, 693, 673, and 653 K.

Table S2. Summary of the RWGS data

Catalyst	d / nm	r_{CO} / mol_{CO} mol_{Mo}^{-1} h^{-1} [a]	S_{CO} / % [c]	S_{CH4} / % [d]	E_a / kJ mol^{-1} [e]
β'-Mo_2C	bulk	15.1	99.8	0.2	64±4
Mo-NP(b)/C	1.4±0.5	174 [b]	99.9	0.1	57±3
Mo_{60}-aggregated/C	1.9±0.7	265 [b]	99.9	0.1	54±2
Mo_{60}/C	1.2±0.3	46.2 [b]	99.8	0.2	100±1
Mo_{28}/C	1.0±0.3	96.2 [b]	99.9	0.1	97±1
Mo_{12}/C	0.8±0.2	92.0 [b]	99.9	0.1	94±2
MoO_2	bulk	2.4	~100	~0	147±20

[a] The generation rate for CO at 713 K. [b] Loading amount of Mo before CHR at 773 K for 30 min. [c] Selectivity for CO. [d] Selectivity for CH_4. The amount of C_2H_4 and C_2H_6 was below detection limit. [e] The activation energy was obtained from the r_{CO} at 713, 693, 673, and 653 K.

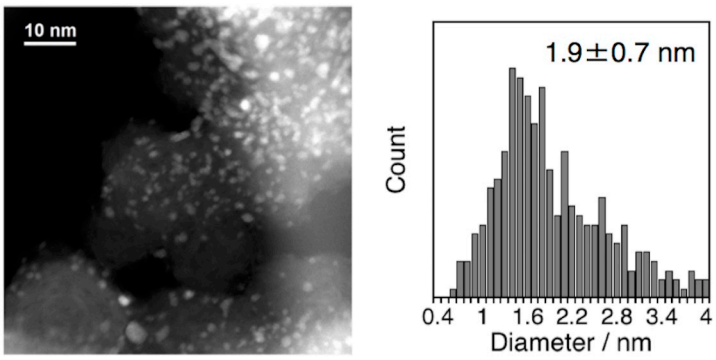

Figure S6. A HAADF-STEM image and a histogram of the particle size distribution of a **Mo_{60}-aggregated/C** after CHR at 773 K for 30 min.

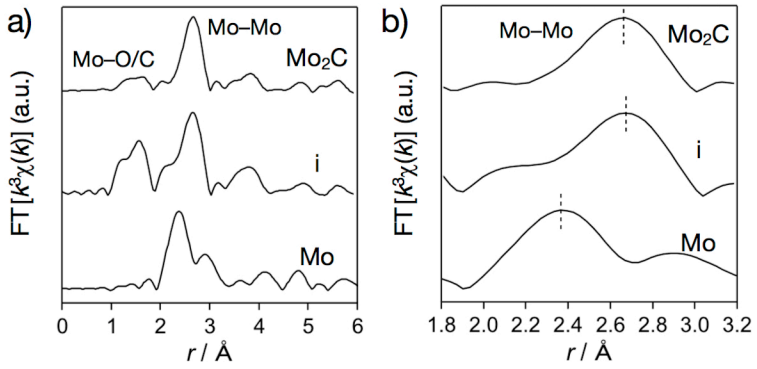

Figure S7. Mo–K edge EXAFS spectra of a) Full range EXAFS spectra and b) magnification of the EXAFS spectra in the region r = 1.8–3.2 Å for i) **Mo_{60}-aggregated/C** after CHR at 773 K for 30 min, together with those of Mo (foil) and β'-Mo_2C.

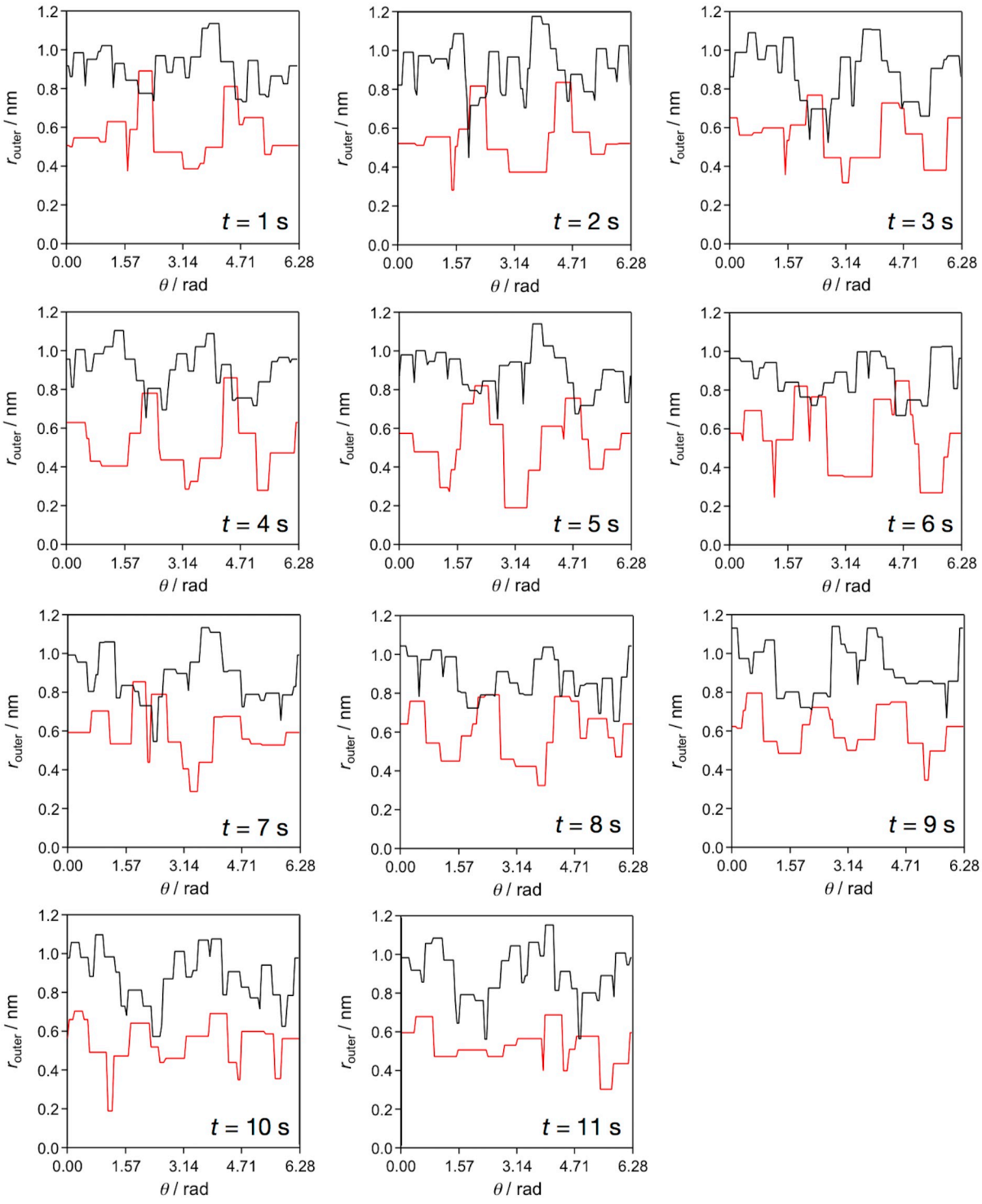

Figure S8. Contour graphs of the polar coordinate with a resolution of 0.05 rad (126 points total) at t = 1–11 s for a) a Mo oxycarbide cluster (red lines) and b) a Mo carbide nanoparticle (black lines) after CHR at 773 K for 30 min, obtained from continuous time-course high-resolution HAADF-STEM images over 11 seconds using an accelerating voltage of 200 kV.

Equation S2. $\Delta\theta$ values were estimated by the following equation, wherein R and r refer to the atomic radius of Mo and the distance between the center of gravity of a particle and the center of Mo atoms, respectively.

$$\Delta\theta = 2\tan^{-1}\frac{R}{r} \qquad \text{(Eq. S2)}$$

Methods

Synthesis of β'-Mo_2C/C. MoO_3 (20 mg) and GMC (20 mg) were grided and mixed in an agate mortar. After applying CHR at 1173 K for 1 h under an H_2 (100 mL min^{-1}) atmosphere on a quartz boat, a black powder (β'-Mo_2C/C) was obtained.

XAFS analyses.[S3] XAFS analyses were carried out using Athena and Artemis[S4] equipped with ATOMS[S5] and FEFF6[S6] in the software package Demeter 0.9.26. XAFS oscillations $\chi(k)$ were extracted using spline smoothing with a Cook-Sayers criterion. The oscillations were normalized using an edge height with its energy dependence. The origin for the photoelectron kinetic energies (E_0) were set at the inflection point of the absorption edge. The curve fitting for EXAFS was applied in k space (k = 3–14 $Å^{-1}$) with equations S3 and S4:

$$\chi(k) = S_0^2 \sum_i \frac{N_i F_i(k) \exp(-2k_i^2 \sigma_i^2)}{k_i r_i^2} \sin\{2k_i r_i + \phi_i(k_i)\} \qquad \text{(Eq. S3)}$$

$$k_i = \sqrt{\frac{2m_e}{\hbar}(E - E_0 - \Delta E_{i0})} \qquad \text{(Eq. S4)}$$

where S_0^2, N_i, σ_i, r_i, $F_i(k_i)$, $\phi_i(k_i)$, and ΔE_{i0} represent the inelastic reduction factor, the coordination number, the Debye-Waller factor, and the bond distance, the backscattering factor, the phase shift, and the difference between experimentally determined E_0 and that used for the theoretical calculation for the i^{th} shell, respectively. $F_i(k_i)$ and $\phi_i(k_i)$ were calculated using FEFF6. FEFF calculations were carried out using a Hedin-Lundqvist potential with maximum effective distance of 3.5 Å for Mo–Mo bonds, and the paths of the single scattering were applied. In each beamline, S_0^2 = 1.0 for Mo–Mo was estimated by using Mo foil, where the coordination numbers are 8 and 6 of bcc Mo. A goodness of the curve fit (R_f) was estimated from equation S5:

$$R_f = \sqrt{\frac{\sum_i k^n \{\chi_i^{data}(k) - \chi_i^{fit}(k,[\alpha])\}^2}{\sum_i \{k^n \chi_i^{data}(k)\}^2}} \qquad \text{(Eq. S5)}$$

where χ_i^{data}, χ_i^{fit}, and [α] reflect the EXAFS functions from measurements, those from calculations, and the fitting parameters, respectively.

Reverse water gas shift reactions. 10–20 mg of the catalyst samples were added into the quartz vessels, respectively. Those samples were pretreated under H_2 flow (1 atm) at 773 K for 10 min, subsequently pretreated under H_2/CO_2 (1/1) flow (1 atm, 20 mL min^{-1}) at 713 K for 1 h. Then, 50-200 μL of the gas samples were extracted using a gas tight syringe after waiting for 20 min every temperature (713, 693, 673, and 653 K), respectively. Those gas samples were analyzed by gas chromatography mass spectrometry (Shimadzu GC-MS QP2020) with a molecular sieve 5A capillary column (Agilent technologies). The amount of CO and CH_4 were detected for m/z = 28 and 15 at the retention time = 1.2 and 0.9 min, respectively, and quantified using those standard gases.

References.

S1. T. Ya. Velikanova, V. Z. Kublii and B. V. Khaenko, *Sov. Powder Metall. Met. Ceram*. 1988, **27**, 891.

S2. Y. Xu, M. Yamazaki and P. Villars, *Jpn. J. Appl. Phys*. 2011, **50**, 11RH02.

S3. The Japanese XAFS society, *Foundations and Applications of XAFS*, Kodansha Ltd. 2017, Chapter 3.

S4. B. Ravela and M. Newville, *J. Synchrotron Rad*. 2005, **12**, 537.

S5. B. Ravel, *J. Synchrotron Rad*. 2001, **8**, 314.

S6. M. Newville, *J. Synchrotron Rad.* 2001, **8**, 322.